Remodeling of Retinal Fatty Acids in an Animal Model of Diabetes

A Decrease in Long-Chain Polyunsaturated Fatty Acids Is Associated With a Decrease in Fatty Acid Elongases Elovl2 and Elovl4

Maria Tikhonenko,[1] Todd A. Lydic,[1] Yun Wang,[2] Weiqin Chen,[3] Madalina Opreanu,[1,4] Andrew Sochacki,[1] Kelly M. McSorley,[1] Rebecca L. Renis,[5] Timothy Kern,[6] Donald B. Jump,[7] Gavin E. Reid,[5,8] and Julia V. Busik[1]

OBJECTIVE—The results of the Diabetes Control and Complications Trial/Epidemiology of Diabetes Interventions and Complications cohort study revealed a strong association between dyslipidemia and the development of diabetic retinopathy. However, there are no experimental data on retinal fatty acid metabolism in diabetes. This study determined retinal-specific fatty acid metabolism in control and diabetic animals.

RESEARCH DESIGN AND METHODS—Tissue gene and protein expression profiles were determined by quantitative RT-PCR and Western blot in control and streptozotocin-induced diabetic rats at 3–6 weeks of diabetes. Fatty acid profiles were assessed by reverse-phase high-performance liquid chromatography, and phospholipid analysis was performed by nano-electrospray ionization tandem mass spectrometry.

RESULTS—We found a dramatic difference between retinal and liver elongase and desaturase profiles with high elongase and low desaturase gene expression in the retina compared with liver. Elovl4, an elongase expressed in the retina but not in the liver, showed the greatest expression level among retinal elongases, followed by Elovl2, Elovl1, and Elovl6. Importantly, early-stage diabetes induced a marked decrease in retinal expression levels of Elovl4, Elovl2, and Elovl6. Diabetes-induced downregulation of retinal elongases translated into a significant decrease in total retinal docosahexaenoic acid, as well as decreased incorporation of very-long-chain polyunsaturated fatty acids (PUFAs), particularly 32:6n3, into retinal phosphatidylcholine. This decrease in n3 PUFAs was coupled with inflammatory status in diabetic retina, reflected by an increase in gene expression of proinflammatory markers interleukin-6, vascular endothelial growth factor, and intercellular adhesion molecule-1.

CONCLUSIONS—This is the first comprehensive study demonstrating diabetes-induced changes in retinal fatty acid metabolism. Normalization of retinal fatty acid levels by dietary means or/and modulating expression of elongases could represent a potential therapeutic target for diabetes-induced retinal inflammation. ***Diabetes*** **59:219–227, 2010**

Early diabetic retinopathy has been suggested to be a low-grade chronic inflammatory disease (1–3) with a number of inflammatory markers, such as vascular endothelial growth factor (VEGF) (4,5), intercellular adhesion molecule (ICAM)-1 (6,7), tumor necrosis factor (TNF)-α (8), and interleukin (IL)-6 (9), shown to be upregulated in diabetic retina. The individual molecular steps leading to inflammation in the retina are not well resolved but likely involve hyperglycemia and dyslipidemia associated with diabetes.

Dyslipidemia is a major metabolic disorder of diabetes, and the Diabetes Control and Complications Trial/Epidemiology of Diabetes Interventions and Complications cohort study revealed that dyslipidemia was significantly associated with the development of diabetic retinopathy (10). Diabetic dyslipidemia is the result of an imbalance in the complex regulation of lipid uptake, metabolism, release by adipocytes, and clearance from circulation (11,12). Fatty acid metabolism perturbation in diabetes is an important part of diabetic dyslipidemia (13).

To understand the effects of diabetes on plasma and tissue fatty acid composition, two metabolic routes have to be considered: de novo lipogenesis and the polyunsaturated fatty acid (PUFA) remodeling Sprecher pathway (14). Saturated fatty acids (SRAs), monounsaturated fatty acids (MUFAs), and PUFAs are synthesized from dietary precursors (glucose, palmitic$_{16:0}$, oleic$_{18:1n9}$, linoleic$_{18:2n6}$, α-linolenic$_{18:3n3}$, eicosapentaenoic acid [EPA$_{20:5n3}$], and docosahexaenoic acid [DHA$_{22:6n3}$]) through a series of desaturation (Δ5-desaturase [Δ5D], Δ6-desaturase [Δ6D], or Δ9-desaturase [Δ9D]) and elongation (Elovl1–7) reactions. In the recent work by Agbaga et al. (15), the Sprecher pathway was expanded to include very-long-chain PUFAs (VLCPUFAs), up to 38 carbon fatty

From the [1]Department of Physiology, Michigan State University, East Lansing, Michigan; [2]GTx, Memphis, Tennessee; the [3]Department of Medicine, Baylor College of Medicine, Houston, Texas; the [4]Department of Microbiology and Molecular Genetics, Michigan State University, East Lansing, Michigan; the [5]Department of Chemistry, Michigan State University, East Lansing, Michigan; the [6]Department of Medicine, Division of Endocrinology, Case Western Reserve University, Cleveland, Ohio; the [7]Linus Pauling Institute, Oregon State University, Corvallis, Oregon; and the [8]Department of Biochemistry and Molecular Biology, Michigan State University, East Lansing, Michigan.

Corresponding author: Julia V. Busik, busik@msu.edu.

Received 4 June 2009 and accepted 9 September 2009. Published ahead of print at http://diabetes.diabetesjournals.org on 29 October 2009. DOI: 10.2337/db09-0728.

M.T. and T.A.L. contributed equally to this work.

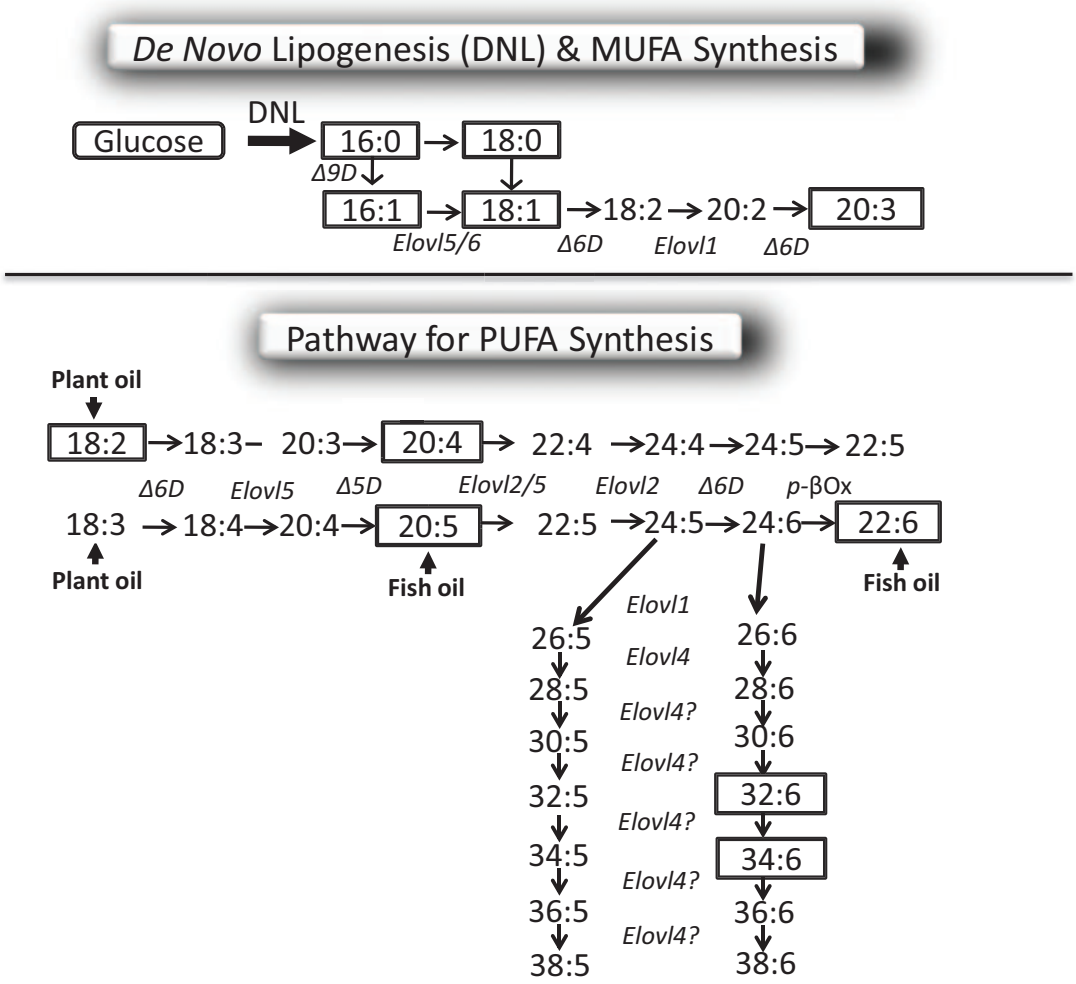

FIG. 1. De novo lipogenesis and PUFA remodeling pathways. Fatty acids are synthesized from glucose through de novo lipogeneses or converted from dietary palmitic$_{16:0}$, oleic$_{18:1n9}$, linoleic$_{18:2n6}$, and α-linolenic$_{18:3n3}$ acids to long-chain unsaturated fatty acids in vivo by a series of desaturation (Δ5-desaturase [Δ5D], Δ6-desaturase [Δ6D], or Δ9-desaturase [Δ9D]) and elongation (Elovl1–7) reactions. Fatty acids that accumulate in animal and human tissues are in solid boxes. Dietary linoleic$_{18:2n6}$ and α-linolenic$_{18:3n3}$ acids are obtained from plants, and EPA$_{20:5n3}$ and DHA$_{22:6n3}$ are rich in fish oil. A recent study demonstrated that Elovl4 is necessary for synthesis of C26 and C28 VLCPUFAs from 24:5n3 and 24:6n3 fatty acid precursors and suggests that Elovl4 is also required for synthesis of >C28 VLCPUFAs. There is no interconversion between n3, n6, and n9 fatty acids in animals.

acids, in which elongation of shorter-chain fatty acids precursors is performed by Elovl4 (Fig. 1). Elovl4 has very limited tissue specificity. It is highly expressed in the retina (16–18), thymus, and skin (17), as well as at lesser levels in the brain (17,18) and testis (18). Elovl4 is not expressed in the liver (17,18). In human retina, Elovl4 was shown to be primarily expressed in the inner segment of photoreceptors extending to photoreceptor cell bodies in the outer nuclear layer (19). Moderate labeling was also observed in the ganglion cells (19). Elovl4 has received much attention recently, as an autosomal-dominant Stargardt-like macular dystrophy was linked to several dominant-negative mutations in Elovl4 (19–21). The role of VLCPUFAs produced by Elovl4 is not known, but because of their localization in retinal outer-segment membranes and their ability to span both leaflets of the lipid bilayer, they are suggested to play a role in stabilizing cellular membranes with high curvature, such as the rims of photoreceptor disks (15). Fatty acid desaturase enzymes are known to be inhibited in diabetes (22–24), and there is emerging information suggesting that certain elongases might also be affected (25). Thus, diabetes may result in reduced fatty acid remodeling and, consequently, lead to an accumulation of the substrates and depletion of the products. The elongases Elovl2 and Elovl6 are ubiquitously expressed in most tissues; however, retina expresses Elovl2 at a very high level. Elovl2 is involved in several steps of DHA$_{22:6n3}$ biosynthesis (26). Retina has a unique fatty acid profile with one of the highest levels of long-chain PUFAs, especially DHA$_{22:6n3}$, in the body (27). We have previously demonstrated that DHA$_{22:6n3}$ has a pronounced anti-inflammatory effect on cytokine-induced activation of the nuclear factor (NF)-κB pathway and adhesion molecule expression in human retinal endothelial cells (HRECs) (28). Thus, perturbation of lipid metabolism in diabetes with a subsequent decrease in DHA$_{22:6n3}$ could create proinflammatory conditions in the retina, potentially contributing to the development of diabetic retinopathy. The effect of diabetes on retinal fatty acid elongases and desaturases and diabetes-induced changes in retinal fatty acid remodeling has not been analyzed and represents one of the goals of this study.

RESEARCH DESIGN AND METHODS

Reagents. High-performance liquid chromatography (HPLC)-grade acetonitrile, acetic acid, methanol, chloroform, streptozotocin (STZ), and commonly used chemicals and reagents were from Sigma-Aldrich Chemical (St. Louis, MO).

Animals and induction of STZ-induced diabetes. Male Sprague-Dawley rats weighing 237–283 g were made diabetic with a single intraperitoneal injection of 65 mg STZ per kg body wt. Body weight gains and blood glucose for the control and STZ-induced diabetic groups were monitored biweekly. At 3–6 weeks after STZ injection, the animals were killed and blood plasma, liver, and retina were recovered for analyses of fatty acid profiles and/or fatty acid elongase and desaturase expression levels. To isolate the retina, the optic nerve was cut out; the eye was opened; the coronary, cornea, and lens were discarded; and the retina was separated from choroid, washed in PBS, and frozen. Rats were maintained on Harlan-Teklad laboratory diet (no. 8,640) and water ad libitum. The fatty acid composition of the diet was analyzed by reverse-phase HPLC (RP-HPLC, see below) and found to be 16:0, 20.0%; 18:0, 1.8%; 18:1n9, 21.9%; 18:2n6, 50.8%; 18:3n3, 5.6%; 18:3n6, 0.1%; 20:4n6, 0.1%; 20:5n3, 0.4%; 22:5n3, 0.1%; and 22:6n3, 0.3%. Animal protocol was approved by the Michigan State University Institutional Animal Care and Use Committee. All experiments followed the guidelines set forth by the Association for Research in Vision and Ophthalmology Resolution on Treatment of Animals in Research.

RNA and protein isolation. Rat tissues were homogenized in Trizol reagent (Invitrogen), and RNA was isolated according to manufacturer instructions. After adding chloroform, the upper aqueous phase was separated and RNA was precipitated with isopropyl alcohol, washed with 75% ethanol, and redissolved in RNase-free water. Proteins from the same samples were isolated by washing in Tris buffer (30 mmol/l Tris-HCl, pH 6.8, with 0.1% SDS) followed by concentration on Amicon-15 (Millipore) centrifugal filters. After concentration, protease/phosphatase inhibitor cocktail was added and samples were frozen until further analysis.

Real-time qRT-PCR. Transcript-specific primers were designed using Primer3 software (available at http://frodo.wi.mit.edu/primer3/). First-strand cDNA was synthesized using the SuperScript II RNase H Reverse Transcriptase (Invitrogen, Carlsband, CA), and PCRs were performed in triplicate as previously described (25). Transcripts of interest were normalized to the abundance of cyclophilin mRNA. Rat gene–specific primers used in this study were Elovl4: GAAGTGGATGAAAGACCGAGA (sense) and GCGTTGTATGATCCCATGAA (antisense); Elovl7: TGGCGTTCAGCGATCT TAC and GATGATGGTTTGTGGCAGAG; IL-6: CCAGGAAATTTGCCTATTGA and GCTCTGAATGACTCTGGCTTT; VEGF A: GCTCTCTTGGGTGCACTGG and CACCACTTCATGGGCTTTCT; and ICAM-1: CCACCATCACTGTGTAT TCGTT and ACGGAGCAGCACTACTGAGA. All other primers for rat elongases and desaturases were described previously (25).

Western blotting. Protein concentration was determined by a Qubit fluorometer (Invitrogen), according to manufacturer's instructions, and equivalent amounts of protein were loaded on the SDS-polyacrylamide (10%) minigels for SDS-PAGE separation. The separated proteins were electrophoretically transferred to a nitrocellulose membrane (Bio-Rad, Hercules, CA), blocked for 30 min at room temperature, and probed with primary rabbit anti-Elovl4 (Abcam) and mouse anti-α tubulin (Sigma) antibody followed by fluorescent secondary antibody (Invitrogen). The blots were analyzed by the Licor Odyssey scanner and quantitated using Licor Odyssey software.

Total lipid extraction. Total lipids from retina, blood plasma, and liver were extracted with chloroform-methanol (2:1, vol/vol), normalized to tissue weight, dried, and resuspended as previously described (29). Acidification of total lipid extracts was omitted, as low pH has been demonstrated to destroy acid-labile plasmalogen lipids (30), which are abundant in neural tissues. No significant decrease of recovery of abundant lipid classes was observed in the absence of pH modification (29). Blood plasma lipids were normalized to protein, as measured by Qubit assay. Erythrocyte total lipids were extracted from 100 mg of packed cells by a modified Rose and Oklander method (31). Briefly, lysed cells were combined with 6.8 ml of 80% 2-propanol, vortexed, and incubated for 1 h on ice with occasional mixing. Lipids were extracted twice by addition of 3.2 ml of 100% chloroform and 1-h incubation on ice, with phase separation after each chloroform addition achieved by centrifugation at 2,000*g* for 30 min. Acidification of the extraction mixture was omitted, as it was found that low pH destroys acid-labile plasmalogen lipids (30), which are abundant in neural tissues. No significant decrease of recovery of abundant lipid classes was observed in the absence of pH modification (29). Pooled lipid extracts were dried, resuspended, and stored as described above.

Lipid analysis by nano-electrospray ionization tandem mass spectrometry. Lipid extracts were introduced to a triple-quadrupole mass spectrometer (Thermo Scientific model TSQ Quantum Ultra, San Jose, CA) for nano-electrospray ionization tandem mass spectrometry (nESI-MS/MS) analysis of lipid species as previously described (29). Identification of phospholipid species by precursor ion and neutral loss scan mode MS/MS was performed according to published methods (29,32). Assignment of phosphatidylcholine (GPCho) acyl substituents was achieved by negative ion mode analysis of corresponding GPCho $[M+Cl]^-$ ions byproduct ion scan mode MS/MS, as well as by precursor ion scanning for m/z corresponding to specific deprotonated fatty acyl ions. Peak finding and correction for ^{13}C isotope effects was performed using the Lipid Mass Spectrum Analysis (LIMSA) software version 1.0 peak model fit algorithm (33). Quantitative analysis of the relative changes in GPCho lipid abundances between control and diabetic samples was achieved by normalization of the peak area of each detected GPCho m/z to that of the $GPCho_{(16:0/16:0)}$ lipid present in each of the samples, after correction for ^{13}C isotope contributions.

Tissue fatty acid analysis by RP-HPLC. An aliquot of total lipids from tissues and blood fractions was saponified (0.4 N KOH in 80% methanol, 50°C for 1 h). Saponified fatty acids were acidified and extracted with diethyl ether (according to Wang et al. [25]) and stored in methanol containing 1 mmol/l butylated hydroxytoluene. Saponified free fatty acids were fractionated and quantitated by RP-HPLC using a YMC J-Sphere (ODS-H80) column and a sigmoidal gradient starting at 86.5% acetonitrile + acetic acid (0.1%) and ending at 100% acetonitrile + acetic acid (0.1%) over 50 min with a flow rate of 1.0 ml/min using a Waters 600 controller. Fatty acids were introduced to the HPLC by injection in methanol and detected using ultraviolet absorbance and evaporative light scatter as previously described (25). Authentic fatty acid standards (Nu-Chek Prep) were used to generate calibration curves for verification and quantification of fatty acids.

Statistical analysis. Data are expressed as the means ± SD. Student's *t* test was used for comparing data obtained from independent samples. Significance was established at $P < 0.05$.

TABLE 1
Body weight gain and blood glucose concentrations of experimental animals

	n	Weight gain (g/day)	Blood glucose (mmol/l)
Control animals	4	4.05 ± 0.65	4.33 ± 0.29
Diabetic animals	7	2.32 ± 0.89	20.80 ± 1.16

Data are means ± SD.

RESULTS

Body weight gain and blood glucose concentration of experimental animals. As presented in Table 1, body weight gain was significantly slower in diabetic animals compared with control animals. Blood glucose levels were almost five times higher in diabetic animals compared with controls. As this was a short-term diabetes study, A1C levels were not measured.

Elongase and desaturase expression level in control and diabetic animals. The gene expression levels of elongases and desaturases in control retinas were determined by quantitative RT-PCR and compared with the levels found in the livers of the same animals. Retinal-specific elongase, Elovl4, had the highest expression level among all the elongases in the retina and was not expressed in the liver. Retinas also had high levels of Elovl2 expression (Fig. 2*A*). Livers exhibited higher levels of Elovl5 and Δ5-, Δ6-, and Δ9-desaturases than retina (Fig. 2*A*), and the liver profile of all elongases and desaturases agreed with our previous study (25).

In the liver, diabetes induced a 25% decrease in Elovl2 and a 33% decrease in Elovl6 expression, as well as an 85% decrease in Δ9-desaturase (Fig. 2*B*) compared with controls. In the retina, diabetes induced a 40% reduction in Elovl4 and 50% reduction in Elovl2 expression levels (Fig. 2*C*). There was no significant effect of diabetes on the retinal desaturases (Fig. 2*C*). A decrease in Elovl4 protein level was confirmed by Western blot, as shown in Fig. 2*D*.

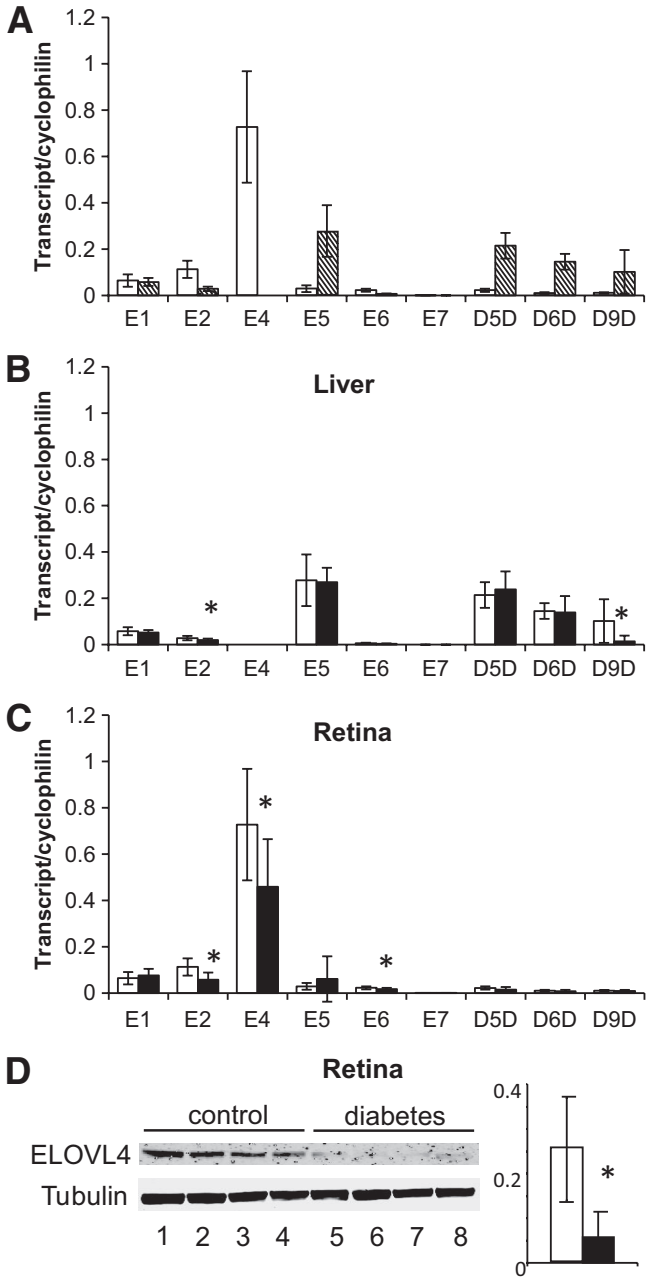

FIG. 2. Expression levels of elongases and desaturases in retinas and livers of control and diabetic animals. Total RNA was extracted from retinas and livers of normal control (n = 4) and STZ-induced diabetic animals (n = 5) after 3–6 weeks of diabetes and analyzed by real-time PCR for elongases 1–7 (E1–7) and Δ5-, Δ6-, and Δ9-desaturase (D5D, D6D, and D9D) expression level. A comparison of the expression levels in retina (□) and liver (▨) of normal control animals is presented in *A*. Diabetes-induced changes in liver elongase and desaturase expression levels are presented in *B* (□, control; ■, diabetes). Diabetes-induced changes in retinal expression levels are presented in *C* (□, control; ■, diabetes). A Western blot of diabetes-induced changes in retina Elovl4 protein level (*lanes 1–4* control, *lanes 5–8* diabetic), and quantification by ratiometric comparison to tubulin, are presented in *D* (□, control; ■, diabetes). Data are presented as means ± SD of five independent experiments. *Statistical significance at $P < 0.05$.

Blood plasma fatty acid profiles of control and diabetic animals. The control and diabetic blood plasma fatty acid profiles 3 weeks after STZ injection are presented in Table 2. There was a tendency toward higher total fatty acids level in diabetic versus control blood plasma. We observed changes in the plasma fatty acid profile consistent with inhibition of fatty acid remodeling in diabetes that leads to a lower end product–to–precursor fatty acid ratio. There was a decrease in two major end products of the PUFA synthesis pathway, arachidonic$_{20:4n6}$ acid and DHA$_{22:6n3}$, relative to their precursors, linoleic$_{18:2n6}$ and α-linolenic$_{18:3n3}$ acid, respectively (Table 2). As a result of these changes, we observed a decrease in unsaturation index (the number of double bonds per fatty acyl residue) and a decrease in long-chain–to–short-chain PUFA ratio in diabetic versus control animals (Table 2).

Liver fatty acid profiles of control and diabetic animals. The control and diabetic liver fatty acid profiles 3 weeks after STZ injection are presented in Table 3. There was an increase in the linoleic acid$_{18:2n6}$ level in the livers of diabetic versus control animals that led to a decrease in long-chain–to–short-chain PUFA ratio (Table 3). There were no other significant changes in liver fatty acid profiles in diabetic versus control animals. The liver unsaturation index and PUFA synthesis pathway end product–to–precursor ratios did not change in diabetic versus control animals (Table 3).

Retinal fatty acid profiles of control and diabetic animals. Retina has a unique fatty acid profile, with the highest content of long-chain PUFAs in the body. In agreement with other studies, retinal profiles were very rich in DHA$_{22:6n3}$ and arachidonic$_{20:4n6}$ acid (Table 4). The levels of linoleic$_{18:2n6}$ and α-linolenic$_{18:3n3}$ acid in the retina were very low; thus we did not calculate the PUFA synthesis pathway end product–to–precursor ratios. Importantly, the retinas of diabetic animals had 28% less DHA$_{22:6n3}$ compared with controls. As a result, we observed a decrease in unsaturation index, a decrease in long-chain–to–short-chain PUFA ratio, and a decrease in the n3-to-n6 PUFA ratio in the retinas of diabetic versus control animals (Table 4). Representative RP-HPLC chromatograms of saponified fatty acids from control and diabetic retina are presented in Fig. 3*A*.

Retinal and erythrocyte phospholipid profiles of control and diabetic animals. In agreement with saponified fatty acid profile data, nESI-MS/MS analysis of the retina lipid extracts of diabetic animals (n = 3) showed a significant (up to 34%) decrease in the abundance of glycerophospholipids containing DHA$_{22:6n3}$ compared with the control animals (n = 3). For example, compare the abundance of the GPCho$_{(18:0/22:6)}$ and GPCho$_{(22:6/22:6)}$ lipids in the ratiometric analysis shown in Fig. 3*B*. Similar decreases in the abundances of DHA$_{22:6n3}$ containing lipids were also observed for glycerophosphoethanolamine and glycerophosphoserine lipids (data not shown). In contrast, an increase (37%) in the abundance of the linoleic$_{18:2n6}$ acid–containing GPCho$_{(16:0/18:2)}$ lipid was observed for the same samples as shown in Fig. 3*B*. In addition to known fatty acids identified by HPLC analysis, nESI-MS/MS analysis revealed several VLCPUFAs, primarily 32:6n3 and 34:6n3, esterified to GPCho in the retina. Interestingly, GPCho$_{(32:6/22:6)}$ was significantly decreased (24%) in diabetic retinas compared with controls, and there was a nonsignificant decrease (9%) of GPCho$_{(34:6/22:6)}$.

In erythrocyte lipid extracts, an increase in the abundance of linoleic$_{18:2n6}$ acid–containing lipids, namely GPCho$_{(16:0/18:2)}$ and GPCho$_{(18:0/18:2)}$, was observed between the diabetic and control samples, consistent with the changes in retina lipids, as shown in Fig. 3*C*. Erythrocytes had very low levels of DHA-containing phospholipid species, and there was no effect of diabetes on these species. There was no detectable GPCho$_{(32:6/22:6)}$ or

TABLE 2
Blood plasma fatty acid profiles of control (n = 4) and diabetic (n = 7) animals

Fatty acids	Blood plasma			P
	Control animals	Diabetic animals	Difference	
Total (nmol/mg protein)	2,262.55 ± 639.64	3,286.54 ± 766.69		0.0972
Mole % of total fatty acids				
16:0 (palmitic)	2.19 ± 1.17	3.70 ± 0.46	↑	0.0362*
18:0 (stearic)	2.25 ± 0.34	2.08 ± 0.40		0.5639
18:1n9 (oleic)	12.65 ± 1.03	13.43 ± 1.74		0.5126
18:2n6 (linoleic)	54.12 ± 2.31	57.44 ± 2.62		0.1207
18:3n3 (α-linolenic)	1.93 ± 0.32	2.71 ± 0.36	↑	0.0214*
18:3n6 (γ-linolenic)	0.31 ± 0.13	0.51 ± 0.37		0.4028
20:3n6 (dihomo-γ-linolenic)	0.84 ± 0.12	0.87 ± 1.15		0.9631
20:3n9 (mead)	0.52 ± 0.32	0.35 ± 0.30		0.4636
20:4n6 (arachidonic)	21.29 ± 2.70	15.90 ± 1.95	↓	0.0161*
20:5n3 (eicosapentaenoic)	0.53 ± 0.08	0.51 ± 0.03		0.7449
22:5n3 (docosapentaenoic)	0.84 ± 0.22	0.54 ± 0.04	↓	0.0235*
22:6n3 (docosahexaenoic)	2.78 ± 0.23	1.72 ± 0.25	↓	0.0010*
Fatty acid ratios				
Unsaturation index	61.58 ± 18.05	38.91 ± 5.56	↓	0.0342*
LCPUFAa/SCPUFAa†	0.48 ± 0.06	0.33 ± 0.05	↓	0.0107*
20:4n6/18:2n6	0.40 ± 0.07	0.28 ± 0.04	↓	0.0232*
22:6n3/18:3n3	1.46 ± 0.17	0.64 ± 0.13	↓	0.0002*

Data are means ± SD. *P < 0.05. †Long-chain PUFAs/short-chain PUFAs.

$GPCho_{(34:6/22:6)}$ in the erythrocytes or in liver and blood plasma (data not shown).

Inflammatory marker expression in control and diabetic retinas. As n3 PUFAs are known to have anti-inflammatory properties, we hypothesized that a decrease in n3 PUFAs would be associated with a proinflammatory state in diabetic retinas. As shown in Fig. 4, diabetic retinas had increased expression levels of several inflammatory markers including adhesion molecules (ICAM-1), cytokines (IL-6), and growth factors (VEGF).

DISCUSSION

The association of dyslipidemia with the development of diabetic retinopathy has been underscored by the Diabetes Control and Complications Trial/Epidemiology of Diabetes Interventions and Complications cohort study (8). Despite this evidence, the experimental data on diabetes-induced changes in lipid profile and lipid metabolism in the retina are not available. This is the first comprehensive study to analyze retinal-specific fatty acid profiles and metabolism and to compare them to liver and blood plasma in control and diabetic animals.

In this study utilizing STZ-induced diabetic rats, we found a decreased level of $DHA_{22:6n3}$, the major retinal long-chain PUFA, in diabetic retina. This finding confirmed earlier studies showing a decrease in relative percentage of $DHA_{22:6n3}$ in the diabetic retina (34,35). In addition to $DHA_{22:6n3}$, VLCPUFAs including 32:6n3 and 34:6n3 were

TABLE 3
Liver fatty acid profiles of control (n = 4) and diabetic (n = 7) animals

Fatty acids	Liver			P
	Control animals	Diabetic animals	Difference	
Total (nmol/mg protein)	1,762.82 ± 480.50	1,357.85 ± 241.19		0.1,542
Mole % of total fatty acids				
16:0 (palmitic)	26.73 ± 8.18	17.55 ± 3.25		0.0518
18:0 (stearic)	11.25 ± 3.74	12.64 ± 3.55		0.9706
18:1n9 (oleic)	3.11 ± 1.03	3.39 ± 1.04		0.4785
18:2n6 (linoleic)	33.14 ± 5.34	39.90 ± 2.71	↑	0.0161*
18:3n3 (α-linolenic)	0.49 ± 0.11	0.59 ± 0.11		0.2101
18:3n6 (γ-linolenic)	0.13 ± 0.14	0.09 ± 0.04		0.2173
20:3n6 (dihomo-γ-linolenic)	0.34 ± 0.04	0.43 ± 0.15		0.3942
20:3n9 (mead)	0.62 ± 0.24	0.51 ± 0.14		0.9340
20:4n6 (arachidonic)	19.87 ± 4.43	21.37 ± 2.50		0.4581
20:5n3 (eicosapentaenoic)	0.15 ± 0.03	0.15 ± 0.05		0.7777
22:5n3 (docosapentaenoic)	0.57 ± 0.15	0.44 ± 0.07		0.2388
22:6n3 (docosahexaenoic)	3.60 ± 0.92	2.94 ± 0.35		0.2294
Fatty acid ratios				
Unsaturation index	5.05 ± 1.82	6.56 ± 1.31		0.0911
LCPUFA/SCPUFA†	0.74 ± 0.07	0.64 ± 0.02	↓	0.0123*
20:4n6/18:2n6	0.60 ± 0.07	0.53 ± 0.03		0.1211
22:6n3/18:3n3	7.74 ± 2.96	5.11 ± 1.05		0.0979

Data are means ± SD. *P < 0.05. †Long-chain PUFAs/short-chain PUFAs.

TABLE 4
Retinal fatty acid profiles of control ($n = 4$) and diabetic ($n = 7$) animals

Fatty acids	Retina			P
	Control animals	Diabetic animals	Difference	
Total (nmol/mg protein)	488.96 ± 17.64	460.32 ± 27.82		0.43
n3 fatty acids	225.1 ± 4.23	166.34 ± 20.66	↓	0.0495*
n6 fatty acids	38.67 ± 4.71	40.59 ± 3.9		0.7693
Mole % of total fatty acids				
16:0 (palmitic)	15.51 ± 0.8	18.32 ± 1.67		0.2046
18:0 (stearic)	18.61 ± 0.97	21.98 ± 2.		0.2046
18:1n9 (oleic)	10.58 ± 0.2	12.9 ± 0.77	↑	0.0441*
18:2n6 (linoleic)	0.44 ± 0.06	0.88 ± 0.05	↑	0.0051*
18:3n3 (α-linolenic)	0.24 ± 0.06	0.17 ± 0.02		0.3556
20:3n6 (dihomo-γ-linolenic)	0.11 ± 0.02	0.04 ± 0.01		0.0819
20:3n9 (mead)	0.97 ± 0.06	1.09 ± 0.2		0.6103
20:4n6 (arachidonic)	7.33 ± 0.75	7.9 ± 0.64		0.6004
20:5n3 (eicosapentaenoic)	0.04 ± 0.02	0.01 ± 0.01		0.2910
22:5n3 (docosapentaenoic)	0.47 ± 0.08	0.28 ± 0.05		0.1129
22:6n3 (docosahexaenoic)	45.37 ± 1.32	35.47 ± 2.71	↓	0.0305*
Fatty acid ratios				
Unsaturation index	20.77 ± 1.63	14.9 ± 2.57		0.1259
LCPUFA/SCPUFA†	80.39 ± 4.86	42.53 ± 3.94	↓	0.0038*
% n3 fatty acids of total	46.12 ± 1.41	35.93 ± 2.77	↓	0.0306*

Data are means ± SD. *$P < 0.05$. †Long-chain PUFAs/short-chain PUFAs.

detected as substituents of retina GPCho. VLCPUFAs were not detected in lipid classes other than GPCho and were only detected in retina. Three weeks of diabetes reduced retinal levels of 32:6n3-GPCho compared with controls. As a result of these changes, the diabetic retina had a lower unsaturation index and lower long-chain–to–short-chain PUFA ratio. Moreover, there was a shift toward n3 PUFA–deficient, n6 PUFA–rich, profile in the diabetic retina.

In general, n6 PUFAs induce, while n3 PUFAs inhibit, inflammation, and the relative amount of these PUFAs plays an important role in the regulation of immunity (36). Our previous studies indicated that treatment of a cell type affected by diabetic retinopathy, HRECs, with n6 PUFA leads to a lipoxygenase-dependent increase in ICAM-1/vascular cell adhesion molecule-1 expression (37). Conversely, we have demonstrated that $DHA_{22:6n3}$ inhibited cytokine-induced activation of the NFκB signaling pathway and adhesion molecule expression in HRECs (28). Thus, a decrease in the n3-to-n6 PUFA ratio in the diabetic retina observed in this study would create proinflammatory conditions potentially contributing to the development of diabetic retinopathy. Indeed, previous studies demonstrated an upregulation in a number of inflammatory markers in the retina early in diabetes: VEGF (4,5), ICAM-1 (6,7), TNF-α (8), and IL-6 (9). ICAM-mediated leukostasis was detected within 1 week of diabetes in rats (38,39). VEGF was shown to increase ICAM expression in retinas of nondiabetic mice (40), and vitreal VEGF levels were found to be correlated with that of IL-6 and severity of diabetic retinopathy in diabetic patients (41).

In this study, we chose a cytokine (IL-6), a growth factor (VEGF), and an adhesion molecule (ICAM-1) as readout of an inflammatory status in the retinas of diabetic animals with decreased n3/n6 PUFAs. mRNA levels of all three markers were elevated in diabetic retinas compared with controls.

Importantly, diabetes induced the most pronounced changes in the retinal fatty acid profile, whereas liver fatty acid profile was only slightly affected, indicating that the disruption of retinal fatty acid metabolism in diabetes might not simply be a result of altered liver metabolism. Moreover, VLCPUFA-containing phospholipids detected in the retina were not present in the liver or erythrocyte total lipids. The fatty acid profile in a particular peripheral tissue depends on two factors: *1*) the profile in circulation due to the diet and liver metabolism and *2*) the ability of a local tissue to remodel fatty acids. Retina has a unique fatty acid profile characterized by one of the highest levels of $DHA_{22:6n3}$ in the body and by the presence of VLCPUFAs (27,42). While the expression level of retinal desaturases was relatively low compared with retinal elongases, it has been reported that retina can synthesize $DHA_{22:6n3}$ from α-$linolenic_{18:3n3}$ acid and $EPA_{20:5n3}$ (43). Although retina may obtain additional $DHA_{22:6n3}$ by uptake from the circulation, changes in the retinal fatty acid profiles of diabetic animals did not mirror changes observed in liver and plasma fatty acid profiles. Thus, a retina-specific decrease in $DHA_{22:6n3}$ in diabetes is likely to be due to changes in retinal fatty acid metabolism.

To determine the effect of diabetes on retinal fatty acid metabolism, we analyzed the level of fatty acid elongase and desaturase gene expression in control and diabetic animals. Retinas had a very high expression level of the retinal-specific elongase, Elovl4, as well as high expression levels of long-chain PUFA elongase Elovl2. Δ5-, Δ6-, and Δ9-desaturase levels were low compared with the liver expression levels. The high levels of Elovl4 and Elovl2 and low levels of desaturases suggest that the retina is preferentially involved in production of very-long-chain fatty acids and exhibits a low level of de novo lipogenesis. The retinal elongase expression profile that we observed likely explains the high level of long-chain PUFAs in the retina compared with liver and blood plasma levels. Elovl2 elongates $C_{20–22}$ fatty acids (44–46). Elovl4 was recently shown to be involved in VLCPUFA synthesis with substrate specificity for $C_{26–36}$ fatty acids (15). The role of VLCPUFAs is not known. Because of their specific presence in tissues with high membrane curvature and their ability to span both leaflets of the lipid bilayer, VLCPUFAs are suggested to play the role of an anchor stabilizing high

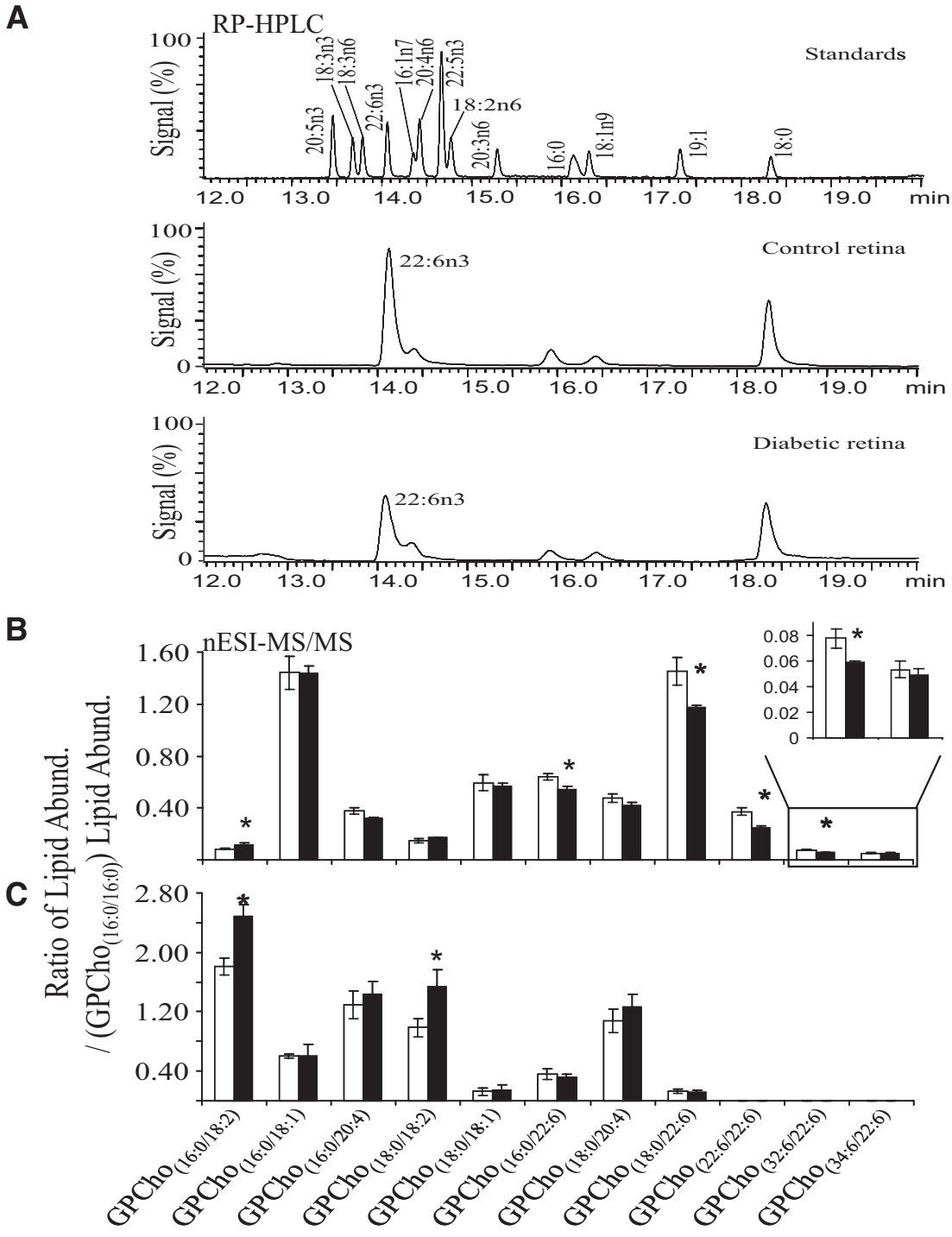

FIG. 3. Fatty acid analysis by RP-HPLC and comparative MS/MS analysis of GPCho lipids in control (n = 3) and diabetic (n = 3) animals at 3–6 weeks post-STZ injection. *A*: Identification and quantification of diabetes-induced changes in total retina saponified fatty acids. *Top*: RP-HPLC chromatogram of a mixture of authentic fatty acid standards. *Middle*: Control retina saponified fatty acids. *Bottom*: Diabetic retina saponified fatty acids. *B*: Ratiometric analysis of changes in GPCho lipid abundance (Abund.) between control (□) and diabetic (■) retina. GPCho species were detected by nESI-MS/MS using PI m/z 184 and further characterized as described in RESEARCH DESIGN AND METHODS. *C*: Ratiometric analysis of changes in GPCho lipid abundance between control and diabetic erythrocytes. Data are presented as means ± SD. *Statistical significance at P < 0.05.

curvature cellular membranes (15). In the retina, VLCPUFAs are mainly present in the rod outer-segment membrane (15), where they are suggested to play a role in stabilizing the rims of photoreceptor disks. This specific localization might explain low abundance of VLCPUFAs in the total retinal lipids extracted in this study. At the same time, specific localization suggests that VLCPUFAs might play an important role in photoreceptor function. This study provides the first direct evidence that a significant decrease in Elovl4 in diabetic retina is indeed associated with a decrease in VLCPUFA (i.e., 32:6n3) synthesis. Despite lower abundance, diabetes-induced decrease in 32:6n3 containing GPCho (24%) was similar to the decrease in $DHA_{22:6n3}$ containing GPChos (15–34%). Elovl4 protein

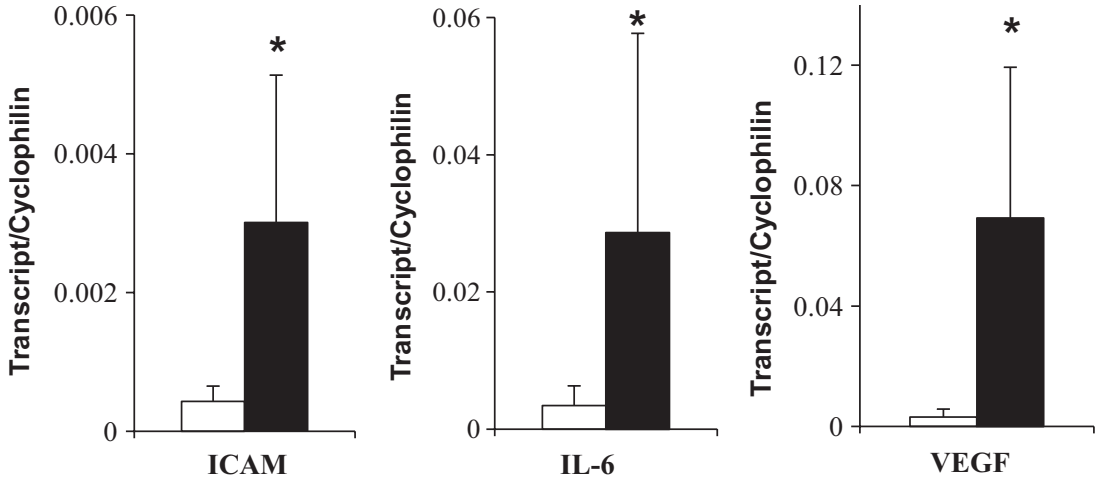

FIG. 4. Expression levels of inflammatory markers in retinas of control (□, $n = 7$) and diabetic (■, $n = 7$) animals. Total RNA was extracted from retinas of control and diabetic animals after 3–6 weeks of diabetes and analyzed by real-time PCR. Diabetes-induced changes in retinal ICAM-1, IL-6, and VEGF expression are shown. Data are presented as means ± SD of at least four independent experiments. *Statistical significance at $P < 0.05$.

expression in diabetic retina was inhibited to a higher degree (73%) compared with mRNA expression (40%), suggesting control of Elovl4 expression at both transcriptional and translational levels. Although decrease of VLCPUFAs is most likely to arise from Elovl4 loss, another plausible explanation could be that this reduction was due to reduction in VLCPUFA precursor lipids, $EPA_{20:5n3}$, and/or $DHA_{22:6n3}$. This possibility can be tested in the future by determining whether downregulation of VLCPUFAs in diabetes persists in animals supplemented with high-$EPA_{20:5n3}$/$DHA_{22:6n3}$ diet.

Another possibility could be that high level of reactive oxygen species in diabetic retina leads to degradation of a highly oxidation-prone DHA molecule. Previous studies using the same STZ-induced diabetic model of similar duration, however, did not find oxidized DHA products in diabetic retina (47).

Several Elovl4 gene mutations have been recently identified in pathogenesis of another retinal disease, Stargardt-like macular dystrophy (19–21). Stargardt-like macular dystrophy is an autosomal-dominant disorder due to a dominant-negative effect of the mutated Elovl4 on wild-type protein (19). As Elovl4 is highly expressed in the photoreceptors (19,21), it is not surprising that mutant Elovl4 transgenic mice are characterized by lipofuscin accumulation, abnormal electrophysiology, and photoreceptor degeneration (20). Although photoreceptors are not the primary site of diabetic retinopathy, several abnormalities in neural retina have been associated with the development of diabetic retinopathy (48,49). The decrease in Elovl4 observed in this study would not be expected to have as dramatic an effect on photoreceptor viability as the dominant-negative mutation in Elovl4. However, the reduction in Elovl4 in diabetic retina could be responsible for more subtle changes in photoreceptor/RPE cell function that could lead to metabolic changes in the whole retina and eventually contribute to the pathology characteristic of diabetic retinopathy.

In conclusion, a decrease in the expression level of retinal fatty acid elongases Elovl2 and Elovl4 and concomitant decrease in the major n3 PUFA, $DHA_{22:6n3}$, as well as the $VLCPUFA_{32:6n3}$, results in an increased n6-to-n3 PUFA ratio in the diabetic retina that likely creates a proinflammatory state contributing to the development of diabetic retinopathy. Increasing the gene expression of fatty acid elongases in the retina represents a potential therapeutic strategy for modulating fatty acid metabolism and altering the pathogenesis of diabetic retinopathy.

ACKNOWLEDGMENTS

This work was supported by grants from the Juvenile Diabetes Research Foundation (2-2005-97 [to J.V.B.]), the National Institutes of Health (EY-016077 [to J.V.B.], R01RR025386 [to G.E.R. and J.V.B.], and DK 43220 [to D.B.J.]), and MAES MICL02163 (to J.V.B.).

No potential conflicts of interest relevant to this article were reported.

REFERENCES

1. Schroder S, Palinski W, Schmid-Schonbein GW. Activated monocytes and granulocytes, capillary nonperfusion, and neovascularization in diabetic retinopathy. Am J Pathol 1991;139:81–100
2. Miyamoto K, Khosrof S, Bursell SE, Rohan R, Murata T, Clermont AC, Aiello LP, Ogura Y, Adamis AP. Prevention of leukostasis and vascular leakage in streptozotocin-induced diabetic retinopathy via intercellular adhesion molecule-1 inhibition. Proc Natl Acad Sci U S A 1999;96:10836–10841
3. Adamis AP. Is diabetic retinopathy an inflammatory disease? Br J Ophthalmol 2002;86:363–365
4. Yang LP, Sun HL, Wu LM, Guo XJ, Dou HL, Tso MO, Zhao L, Li SM. Baicalein reduces inflammatory process in a rodent model of diabetic retinopathy. Invest Ophthalmol Vis Sci 2009;50:2319–2327
5. Sone H, Kawakami Y, Okuda Y, Sekine Y, Honmura S, Matsuo K, Segawa T, Suzuki H, Yamashita K. Ocular vascular endothelial growth factor levels in diabetic rats are elevated before observable retinal proliferative changes. Diabetologia 1997;40:726–730
6. Nozaki M, Ogura Y, Hirabayashi Y, Saishin Y, Shimada S. Enhanced expression of adhesion molecules of the retinal vascular endothelium in spontaneous diabetic rats. Ophthalmic Res 2002;34:158–164
7. Al-Shabrawey M, Rojas M, Sanders T, Behzadian A, El-Remessy A, Bartoli M, Parpia AK, Liou G, Caldwell RB. Role of NADPH oxidase in retinal vascular inflammation. Invest Ophthalmol Vis Sci 2008;49:3239–3244
8. Joussen AM, Poulaki V, Mitsiades N, Kirchhof B, Koizumi K, Dohmen S, Adamis AP. Nonsteroidal anti-inflammatory drugs prevent early diabetic retinopathy via TNF-alpha suppression. FASEB J 2002;16:438–440
9. Gustavsson C, Agardh CD, Hagert P, Agardh E. Inflammatory markers in nondiabetic and diabetic rat retinas exposed to ischemia followed by reperfusion. Retina 2008;28:645–652
10. Lyons TJ, Jenkins AJ, Zheng D, Lackland DT, McGee D, Garvey WT, Klein

RL. Diabetic retinopathy and serum lipoprotein subclasses in the DCCT/EDIC cohort. Invest Ophthalmol Vis Sci 2004;45:910–918
11. Coppack SW, Evans RD, Fisher RM, Frayn KN, Gibbons GF, Humphreys SM, Kirk ML, Potts JL, Hockaday TD. Adipose tissue metabolism in obesity: lipase action in vivo before and after a mixed meal. Metabolism 1992;41:264–272
12. Weinstock PH, Levak-Frank S, Hudgins LC, Radner H, Friedman JM, Zechner R, Breslow JL. Lipoprotein lipase controls fatty acid entry into adipose tissue, but fat mass is preserved by endogenous synthesis in mice deficient in adipose tissue lipoprotein lipase. Proc Natl Acad Sci U S A 1997;94:10261–10266
13. Julius U. Influence of plasma free fatty acids on lipoprotein synthesis and diabetic dyslipidemia. Exp Clin Endocrinol Diabetes 2003;111:246–250
14. Sprecher H, Chen Q. Polyunsaturated fatty acid biosynthesis: a microsomal-peroxisomal process. Prostaglandins Leukot Essent Fatty Acids 1999;60:317–321
15. Agbaga MP, Brush RS, Mandal MN, Henry K, Elliott MH, Anderson RE. Role of Stargardt-3 macular dystrophy protein (ELOVL4) in the biosynthesis of very long chain fatty acids. Proc Natl Acad Sci U S A 2008;105:12843–12848
16. Lagali PS, Liu J, Ambasudhan R, Kakuk LE, Bernstein SL, Seigel GM, Wong PW, Ayyagari R. Evolutionarily conserved ELOVL4 gene expression in the vertebrate retina. Invest Ophthalmol Vis Sci 2003;44:2841–2850
17. Umeda S, Ayyagari R, Suzuki MT, Ono F, Iwata F, Fujiki K, Kanai A, Takada Y, Yoshikawa Y, Tanaka Y, Iwata T. Molecular cloning of ELOVL4 gene from cynomolgus monkey (Macaca fascicularis). Exp Anim 2003;52:129–135
18. Zhang XM, Yang Z, Karan G, Hashimoto T, Baehr W, Yang XJ, Zhang K. Elovl4 mRNA distribution in the developing mouse retina and phylogenetic conservation of Elovl4 genes. Mol Vis 2003;9:301–307
19. Grayson C, Molday RS. Dominant negative mechanism underlies autosomal dominant Stargardt-like macular dystrophy linked to mutations in ELOVL4. J Biol Chem 2005;280:32521–32530
20. Karan G, Lillo C, Yang Z, Cameron DJ, Locke KG, Zhao Y, Thirumalaichary S, Li C, Birch DG, Vollmer-Snarr HR, Williams DS, Zhang K. Lipofuscin accumulation, abnormal electrophysiology, and photoreceptor degeneration in mutant ELOVL4 transgenic mice: a model for macular degeneration. Proc Natl Acad Sci U S A 2005;102:4164–4169
21. Zhang K, Kniazeva M, Han M, Li W, Yu Z, Yang Z, Li Y, Metzker ML, Allikmets R, Zack DJ, Kakuk LE, Lagali PS, Wong PW, MacDonald IM, Sieving PA, Figueroa DJ, Austin CP, Gould RJ, Ayyagari R, Petrukhin K. A 5-bp deletion in ELOVL4 is associated with two related forms of autosomal dominant macular dystrophy. Nat Genet 2001;27:89–93
22. Brenner RR. Hormonal modulation of delta6 and delta5 desaturases: case of diabetes. Prostaglandins Leukot Essent Fatty Acids 2003;68:151–162
23. Nakamura MT, Nara TY. Gene regulation of mammalian desaturases. Biochem Soc Trans 2002;30:1076–1079
24. Rimoldi OJ, Finarelli GS, Brenner RR. Effects of diabetes and insulin on hepatic delta6 desaturase gene expression. Biochem Biophys Res Commun 2001;283:323–326
25. Wang Y, Botolin D, Xu J, Christian B, Mitchell E, Jayaprakasam B, Nair MG, Peters JM, Busik JV, Olson LK, Jump DB. Regulation of hepatic fatty acid elongase and desaturase expression in diabetes and obesity. J Lipid Res 2006;47:2028–2041
26. Meyer A, Kirsch H, Domergue F, Abbadi A, Sperling P, Bauer J, Cirpus P, Zank TK, Moreau H, Roscoe TJ, Zahringer U, Heinz E. Novel fatty acid elongases and their use for the reconstitution of docosahexaenoic acid biosynthesis. J Lipid Res 2004;45:1899–1909
27. Anderson RE. Lipids of ocular tissues: IV. A comparison of the phospholipids from the retina of six mammalian species. Exp Eye Res 1970;10:339–344
28. Chen W, Esselman WJ, Jump DB, Busik JV. Anti-inflammatory effect of docosahexaenoic acid on cytokine-induced adhesion molecule expression in human retinal vascular endothelial cells. Invest Ophthalmol Vis Sci 2005;46:4342–4347
29. Lydic TA, Busik JV, Esselman WJ, Reid GE. Complementary precursor ion and neutral loss scan mode tandem mass spectrometry for the analysis of glycerophosphatidylethanolamine lipids from whole rat retina. Anal Bioanal Chem 2009;394:267–275
30. Murphy EJ, Stephens R, Jurkowitz-Alexander M, Horrocks LA. Acidic hydrolysis of plasmalogens followed by high-performance liquid chromatography. Lipids 1993;28:565–568
31. Rose H, Oklander M. An improved method for the extraction of lipids from human erythrocytes. J Lipid Res 1965;6:428–443
32. Han X, Gross RW. Shotgun lipidomics: electrospray ionization mass spectrometric analysis and quantitation of cellular lipidomes directly from crude extracts of biological samples. Mass Spectrom Rev 2005;24:367–412
33. Haimi P, Uphoff A, Hermansson M, Somerharju P. Software tools for analysis of mass spectrometric lipidome data. Anal Chem 2006;78:8324–8331
34. Futterman S, Sturtevant R, Kupfer C. Effect of alloxan diabetes on the fatty acid composition of the retina. Invest Ophthalmol 1969;8:542–544
35. Hegde KR, Varma SD. Electron impact mass spectroscopic studies on mouse retinal fatty acids: effect of diabetes. Ophthalmic Res 2009;42:9–14
36. Harbige LS. Fatty acids, the immune response, and autoimmunity: a question of n-6 essentiality and the balance between n-6 and n-3. Lipids 2003;38:323–341
37. Chen W, Jump DB, Grant MB, Esselman WJ, Busik JV. Dyslipidemia, but not hyperglycemia, induces inflammatory adhesion molecules in human retinal vascular endothelial cells. Invest Ophthalmol Vis Sci 2003;44:5016–5022
38. Joussen AM, Poulaki V, Qin W, Kirchhof B, Mitsiades N, Wiegand SJ, Rudge J, Yancopoulos GD, Adamis AP. Retinal vascular endothelial growth factor induces intercellular adhesion molecule-1 and endothelial nitric oxide synthase expression and initiates early diabetic retinal leukocyte adhesion in vivo. Am J Pathol 2002;160:501–509
39. Joussen AM, Murata T, Tsujikawa A, Kirchhof B, Bursell SE, Adamis AP. Leukocyte-mediated endothelial cell injury and death in the diabetic retina. Am J Pathol 2001;158:147–152
40. Lu M, Perez VL, Ma N, Miyamoto K, Peng HB, Liao JK, Adamis AP. VEGF increases retinal vascular ICAM-1 expression in vivo. Invest Ophthalmol Vis Sci 1999;40:1808–1812
41. Funatsu H, Yamashita H, Shimizu E, Kojima R, Hori S. Relationship between vascular endothelial growth factor and interleukin-6 in diabetic retinopathy. Retina 2001;21:469–477
42. Fliesler SJ, Anderson RE. Chemistry and metabolism of lipids in the vertebrate retina. Prog Lipid Res 1983;22:79–131
43. Delton-Vandenbroucke I, Grammas P, Anderson RE. Polyunsaturated fatty acid metabolism in retinal and cerebral microvascular endothelial cells. J Lipid Res 1997;38:147–159
44. Moon YA, Shah NA, Mohapatra S, Warrington JA, Horton JD. Identification of a mammalian long chain fatty acyl elongase regulated by sterol regulatory element-binding proteins. J Biol Chem 2001;276:45358–45366
45. Jakobsson A, Westerberg R, Jacobsson A. Fatty acid elongases in mammals: their regulation and roles in metabolism. Prog Lipid Res 2006;45:237–249
46. Leonard AE, Pereira SL, Sprecher H, Huang YS. Elongation of long-chain fatty acids. Prog Lipid Res 2004;43:36–54
47. Sunada S, Kiyose C, Kubo K, Takebayashi J, Sanada H, Saito M. Effect of docosahexaenoic acid intake on lipid peroxidation in diabetic rat retina under oxidative stress. Free Radic Res 2006;40:837–846
48. Barber AJ, Lieth E, Khin SA, Antonetti DA, Buchanan AG, Gardner TW. Neural apoptosis in the retina during experimental and human diabetes: early onset and effect of insulin. J Clin Invest 1998;102:783–791
49. Gardner TW, Antonetti DA, Barber AJ, LaNoue KF, Nakamura M. New insights into the pathophysiology of diabetic retinopathy: potential cell-specific therapeutic targets. Diabetes Technol Ther 2000;2:601–608